



- 1 Improved Runoff Simulations for a Highly Varying Soil Depth and Complex Terrain
2 Watershed in the Loess Plateau with Community Land Model Version 5
3 Jiming Jin^{1†}, Lei Wang^{2,3†}, Jie Yang^{2,3}, Bingcheng Si⁴, and Guoyue Niu^{5,6}
4 ¹College of Resources and Environment, Yangtze University, Wuhan 430100, Hubei,
5 China
6 ²College of Water Resources and Architectural Engineering, Northwest A & F
7 University, Yangling 712100, Shaanxi, China
8 ³Key Laboratory of Agricultural Soil and Water Engineering in Arid and Semiarid Areas,
9 Ministry of Education, Northwest A & F University, Yangling 712100, Shaanxi, China
10 ⁴Department of Soil Science, University of Saskatchewan, Saskatoon, SK S7N 5A8,
11 Canada
12 ⁵Biosphere 2, the University of Arizona, Tucson, AZ 85623, USA
13 ⁶Department of Hydrology and Water Resources, University of Arizona, Tucson, AZ
14 85721, USA
15 Correspondence: Jiming Jin (jimingjin99@gmail.com)
16 † These authors contributed equally to this study



17 Abstract. This study aimed to improve runoff simulations and explore deep soil
18 hydrological processes for a watershed in the center of the Loess Plateau (LP), China.
19 This watershed, the Wuding River Basin (WRB), has very complex topography, with
20 soil depths ranging from 0 to 197 m. The hydrological model used for our simulations
21 was Community Land Model version 5 (CLM5) developed by the National Center for
22 Atmospheric Research. Actual soil depths and river channels were incorporated into
23 CLM5 to realistically represent the physical features of the WRB. Through sensitivity
24 tests, CLM5 with 150 soil layers produced the most reasonable results and was adopted
25 for this study. Our results showed that CLM5 with actual soil depths significantly
26 suppressed unrealistic variations of the simulated sub-surface runoff when compared to
27 the default simulations with a fixed soil depth of 8 m. In addition, CLM5 with higher-
28 resolution soil layering slightly improved runoff simulations, but generated simulations
29 with much smoother vertical water flows that were consistent with the uniform
30 distribution of soil textures in our study watershed. The runoff simulations were further
31 improved by the addition of river channels to CLM5, where the seasonal variability of
32 the simulated runoff was reasonably captured. Moreover, the magnitude of the
33 simulated runoff remarkably decreased with increased soil evaporation by lowering the
34 soil water content threshold, which triggers surface resistance. The lowered threshold
35 was consistent with the loess soil, which has a high sand component. Such soils often
36 generate stronger soil evaporation than soils dominated by clay. Finally, with the above
37 changes in CLM5, the simulated total runoff matched very closely with observations.
38 When compared with those for the default runoff simulations, the correlation coefficient,
39 root-mean-square error, and Nash Sutcliffe coefficient for the improved simulations
40 changed dramatically from 0.02, 10.37 mm, and -12.34 to 0.62, 1.8 mm, and 0.61. The
41 results in this study provide strong physical insight for further investigation of



42 hydrological processes in complex terrain with deep soils.

43 Key words: CLM5, complex terrain, soil depth, runoff

44

45 1 Introduction

46 Understanding runoff processes in regions with very complex topography is important
47 to managing and predicting water resources. Such an understanding can assist in
48 quantifying the allocation of water resources (Chen et al., 2013; Camacho et al., 2015),
49 evaluating surface and groundwater vulnerability to natural and anthropogenic
50 processes (Uhlenbrook et al., 2002), improving drought and flood management
51 (Camacho et al., 2015), and predicting the amount and spatiotemporal distribution of
52 water resources (Saraiva Okello et al., 2018). However, complex topography leads to
53 intricate runoff processes (Jencso et al., 2011), causing uncertain estimation of water
54 resources. Therefore, it is crucial to investigate runoff processes for the well-being of
55 topographically complex regions.

56

57 As the largest area covered by continuous loess soils in the world (Fu et al., 2017; Zhu
58 et al., 2018), the Loess Plateau (LP) in China has complicated hydrological processes
59 because of its extremely complex topography and unique soil types. Due to an arid and
60 semi-arid climate and a population of more than 100 million (Zhang et al., 2018), this
61 region experiences severe water shortages (Xiao et al., 2019). It is essential to
62 accurately estimate the spatiotemporal distribution of water resources in this region of
63 complex terrain. Soil depth in the LP can reach 350 m (Zhu et al., 2018; Li et al., 2019),
64 making it difficult to measure deep soil hydrological processes and understand runoff
65 generation (Shao et al., 2018; Liu et al., 2012). In addition, terrain in the LP includes
66 loess tablelands, ridges, hills, gullies, and river channels (Fu, 1989), all of which have



67 quite different runoff generation processes (Liu et al., 2012). In loess tablelands with
68 deep water tables (Huang et al., 2013; Shao et al., 2018), the soils store most infiltrated
69 water, generate insignificant surface runoff, and remarkably delay sub-surface runoff.
70 Areas in the LP with gullies and river channels usually have high water tables (Liu et
71 al., 2012) and can easily be saturated during precipitation events, generating a large
72 amount of surface runoff. In the meantime, the loess soils that dominate the LP have a
73 large capillary porosity, with loose and homogeneous textures due to a high sand
74 component, often resulting in high evaporation (Li et al., 1985; Lei, 1987; Han et al.,
75 1990; Wang and Shao, 2013). A better understanding of the hydrological processes
76 within the complex terrain and special soil types of the LP is vital to improving the
77 prediction of water resources in this region.

78
79 Numerical hydrological models are essential tools to investigate runoff processes in the
80 LP. Field measurements such as those from tracer techniques (Huang et al., 2011; Li et
81 al., 2017; Huang et al., 2017; Huang et al., 2019; Xiang et al., 2019) have been made to
82 quantify the hydrological processes in the LP, but these measurements have significant
83 limitations, including short temporal and small spatial coverage, which cannot account
84 for the processes at watershed scales. Hydrological models based on mass and energy
85 equations are effective in simulating the long-term spatiotemporal variability of runoff
86 at watershed scales (Döll and Fiedler, 2007; Turkeltaub et al., 2015; Shao et al., 2018).
87 Based on detailed soil information at a depth of 98 m at a research site on the Changwu
88 tableland in the LP, Shao et al. (2018) used a hydrological model to generate reasonable
89 simulations for deep soil percolation and groundwater level. Their study provides
90 important clues (e.g., high-resolution soil layering) for exploring deep soil hydrological
91 processes and producing reliable runoff simulations at a watershed scale in the LP.



92 Therefore, it is apparent that hydrological models can overcome the drawbacks of field
93 experiments.

94
95 However, in hydrological models, soil depth and river channels are very important in
96 simulating soil water movement and storage and runoff processes, especially in regions
97 with complex topography (Tesfa et al., 2009; Fu et al., 2011). Soil depth is set to a
98 constant in most hydrological models (Shangguan et al., 2017). For example, in the
99 Community Land Model version 5 (CLM5; Lawrence et al., 2018), soil depth is set to
100 about 8 m, and the Noah (Ek et al., 2003) and Noah MP (Niu et al., 2011) models have
101 a soil depth of 2 m, which cannot represent the realistic spatial distribution of soil depth
102 in the LP, which ranges from 0 to 350 m. In addition, soil depth in most river channels
103 with exposed bedrock in the LP is close to zero (Jing and Cheng, 1983; Li et al., 2017;
104 Zhu et al., 2018), and areas dominated by these channels are very important in
105 generating runoff. Some hydrological models such as CLM5 and the Soil and Water
106 Assessment Tool (Neitsch et al., 2011) have embedded river routing schemes. In these
107 schemes, the river channels described based on elevation differences still have the same
108 soil depth as other places without these channels, which cannot reflect the actual
109 conditions in the LP and many other regions where soil depth changes significantly
110 across rivers. Thus, soil depth variations and river channels need to be considered in
111 hydrological models for better soil water flow and runoff simulations.

112
113 The objective of this study was to use CLM5 to improve runoff simulations and better
114 understand the hydrological processes with varying soil depths for a very complex
115 topography watershed in the LP. To achieve this objective, the highly varying soil
116 depths and river channels were incorporated into CLM5 to realistically represent the



117 features of the watershed. In fact, Brunke et al. (2016) have conducted a study with
118 CLM version 4.5 by including varying soil depths at a global scale where the runoff
119 simulations are focused at grid cell scales, which cannot be evaluated with actual
120 streamflow data. However, evaluating hydrological simulations at watershed scales is
121 essential to improving our understanding of runoff processes. In this study, the most
122 important finding was that river channels where the soil depth is often equal or close to
123 zero played a vital role in runoff simulations especially in complex topography areas.
124 According to our extensive literature search, river channels are not configured in most
125 of existing land surface and hydrological models. In addition, although this study
126 focused on a relatively small watershed, our runoff simulation methods and science
127 ideas can be easily transferred to investigate the hydrological processes in other
128 watersheds across the world with observed soil depth and river channel information.
129 The text is laid out as follows: Sections 2 and 3 introduce the study area and data,
130 respectively, Section 4 provides the model description, Section 5 describes the
131 methodology, Section 6 includes the results, and the conclusions are in Section 7.

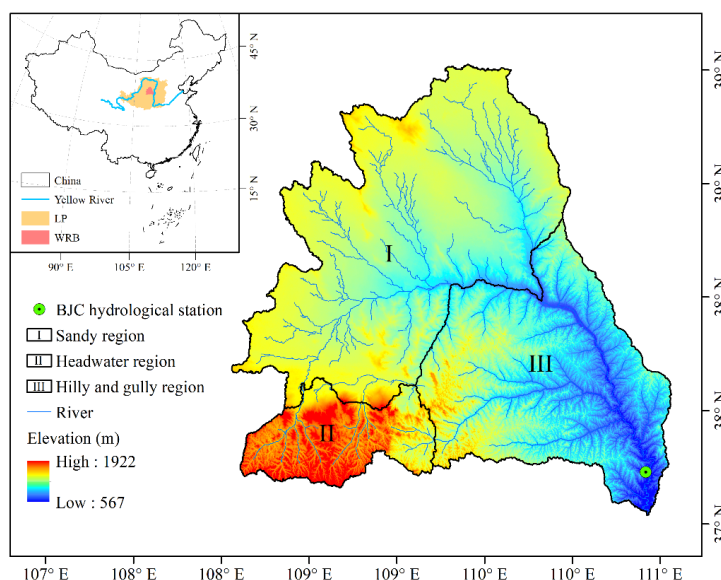
132

133 2 Study Area

134 The WRB was selected as the study area. This basin, with an area of about 30,261 km²,
135 is in the center of the LP (Figure 1), which is the largest continuous loess area in the
136 world (~640,000 km²) (Fu et al., 2017; Zhu et al., 2018). The WRB shows complex
137 geomorphic characteristics including tablelands, ridges, hills, gullies, and river
138 channels (Liu et al., 2012). The main land use types in the WRB are bare ground,
139 grassland, and sparse forest. Across the basin, soil thickness generally ranges from 0 to
140 200 m (Liu, 2016), and the loess, consisting mainly of silt and sand (Li et al., 1985), is
141 relatively homogeneous in the vertical direction (Huang et al., 2013; Xiang et al., 2019).



142 The WRB has a continental monsoon climate with mean annual precipitation of around
143 400 mm, about 70% of which falls during the flood season from June through
144 September, based on observations over the period of 1956-2010 (<http://data.cma.cn/>).
145



146
147 Figure 1. Location of the Loess Plateau (LP) and Wuding River Basin (WRB) in China.
148

149 3 Data

150 3.1 Meteorological and runoff data

151 High-quality meteorological and runoff data for the WRB were used to force and
152 evaluate CLM5, respectively. The Global Soil Wetness Project phase 3 (GSWP3)
153 meteorological dataset (<http://hydro.iis.u-tokyo.ac.jp/GSWP3/index.html>) was selected
154 to drive the model for this study. The GSWP3 dataset contains seven climate forcing
155 variables, including precipitation, air temperature, downward shortwave and longwave
156 radiation, specific humidity, surface pressure, and wind speed. These data cover the
157 period of 1901-2010 with a spatial resolution of 0.5° at a 3-hour time step. Meanwhile,
158 we obtained the observed monthly runoff data of the Baijiachuan (BJC) hydrological



159 station from the Data Sharing Network of Earth System Science
160 (<http://loess.geodata.cn/index.html>). The BJC station is located at the WRB outlet and
161 its drainage area covers ~98% of the basin. These runoff data were used to assess CLM5
162 output.

163

164 3.2 Soil data

165 Soil depth data for the WRB were obtained from different sources. We first collected
166 and recorded 61 soil depths for the WRB and nearby areas from ~15 published papers
167 and books (not cited here). In addition, two soil depth maps for the WRB were obtained
168 from Qi et al. (1991) and Wang (2016) and were digitized. Soil depth data for model
169 grids with gullies and rivers were derived based on digital elevation model (DEM) data.
170 Soil depth in gullies and rivers was assumed to be 0 due to the exposure of bedrock
171 (Jing and Cheng, 1983; Li et al., 2017; Zhu et al., 2018). The elevations of these gully
172 and river channels were retrieved from a DEM at a resolution of 90 m. The differences
173 between these elevations and those at a 5 km resolution were used to represent the soil
174 depth in model grids with gullies and rivers. The proportion of the total gully and river
175 area to the entire WRB area (defined as P_{gr} hereafter) was determined with the
176 Cressman method (Cressman, 1959). A value of 0.3 is suggested by Qi et al. (1991) for
177 the LP. In this study, we identified the optimal P_{gr} value through sensitivity tests by
178 setting different interpolation radii in the Cressman method. The soil depth data from
179 these sources were then combined and interpolated into a 5 km resolution, still based
180 on the Cressman method.

181

182 Soil texture data for the WRB were necessary input into CLM5. These data were
183 derived from a soil type map for the LP (<http://loess.geodata.cn>) and included three soil



184 layers: 0-20, 20-76, and 76-180 cm. For soil layers deeper than 180 cm, the texture data
185 for the 76-180 cm layer were applied.

186

187 4 Model description

188 CLM5 was used in this study for runoff simulations. This model was developed by the
189 National Center for Atmospheric Research. The CLM5 includes one vegetation layer,
190 up to five snow layers, and 20 soil layers. In the model, each grid cell is split into
191 different land units including vegetated surface, lake, urban, glacier, and cropland. The
192 spatial distribution and seasonal climatology of the plant functional types for CLM5 are
193 derived from MODIS satellite land-surface data products (Lawrence and Chase, 2007).
194 CLM5 uses the simplified TOPMODEL (Niu et al., 2005) to parameterize runoff, which
195 is partitioned into surface and sub-surface runoff. Surface runoff is calculated based on
196 the saturation-excess mechanism. Sub-surface runoff is produced when saturated
197 conditions occur within the soil column.

198

199 In CLM5, soil evaporation is affected by soil resistance, which is associated with a dry
200 surface layer (DSL) (Swenson and Lawrence, 2014). A DSL forms near the soil surface
201 in the model when the soil water content in the top layer is below a threshold value
202 (SWC_{th}), which is set to 80% of the soil porosity of the top layer ($SWC_{sat,1}$). The
203 formation of the DSL generates soil resistance, limiting soil evaporation. Meanwhile,
204 CLM5 uses Richard's equation and Darcy's law to describe changes in soil water
205 content (SWC) and soil water flux. The soil hydraulic conductivity and retention used
206 in these equations are determined by the soil texture and the SWC of the previous time
207 step, based on Clapp and Hornberger (1978), Cosby et al. (1984), and Lawrence and
208 Slater (2007).



209

210 5 Methodology

211 5.1 Soil layering

212 As mentioned, soil depth in the WRB is strongly variable, with a range of 0-200 m.

213 However, the default soil depth in CLM5 is set to a constant of 8.03 m and is discretized

214 into 20 layers defined as hydrological active layers (HALs) to distinguish them from

215 the five bedrock layers set in the model. Thus, the settings of this model are not suitable

216 for applications in the WRB. In this study, we changed the soil depth to a variable for

217 the WRB based on the soil depth data discussed previously. Eight sensitivity tests were

218 conducted with soil layer numbers (SLNs) of 20, 50, 75, 100, 125, 150, 175, and 200

219 to determine the optimal soil layering method for runoff simulations in the WRB

220 (Tables 1a and 1b). In each sensitivity test, the SLN is the same for the entire WRB,

221 and the HAL number is identified based on the input soil depth for each soil column.

222 Layers that are not HALs are treated as bedrock layers and are not used in the hydrology

223 calculations in the model.

224 Table 1a. Thickness (m) of each soil layer for different SLNs (20, 50, 75, and 100)

Sequence	SLN				Sequence	SLN			
	20	50	75	100		20	50	75	100
1	0.02	0.02	0.02	0.02	18-20	40.00	2.00	1.00	0.64
2	0.04	0.04	0.04	0.04	21-25		4.00	1.00	0.84
3	0.06	0.06	0.06	0.06	26-35		4.00	2.00	1.04
4	0.08	0.08	0.08	0.08	36-40		6.00	2.00	1.04
5	0.12	0.12	0.12	0.12	41-45		8.00	2.50	1.44
6	0.16	0.16	0.16	0.16	46-50		10.00	3.00	1.44
7	0.20	0.20	0.20	0.20	51-55			3.00	1.44
8	0.24	0.24	0.24	0.24	56-65			4.00	2.00
9	0.28	0.28	0.28	0.28	66			5.14	2.40
10	0.32	0.32	0.32	0.32	67-70			6.00	2.40
11	0.64	0.64	0.64	0.64	71-75			8.00	2.40
12	2.00	1.00	0.80	0.64	76-85				2.80
13	4.84	1.00	0.80	0.64	86-89				4.00
14	12.00	1.04	0.80	0.64	90				4.68
15	16.00	1.80	0.80	0.64	91-95				5.00
16-17	20.00	2.00	1.00	0.64	96-100				6.00

225



226

227 Table 1b. Thickness (m) of each soil layer for different SLNs (125, 150, 175, and 200)

Sequence	SLN				Sequence	SLN			
	125	150	175	200		125	150	175	200
1	0.02	0.02	0.02	0.02	51-70	1.14	1.14	1.14	1.04
2	0.04	0.04	0.04	0.04	71	1.58	1.40	1.20	1.04
3	0.06	0.06	0.06	0.06	72-79	2.00	1.40	1.20	1.04
4	0.08	0.08	0.08	0.08	80-85	2.00	1.50	1.20	1.04
5	0.12	0.12	0.12	0.12	86-100	2.40	1.60	1.20	1.04
6	0.16	0.16	0.16	0.16	101	2.40	1.60	1.20	1.02
7	0.20	0.20	0.20	0.20	102-104	2.40	1.60	1.20	1.14
8	0.24	0.24	0.24	0.24	105	2.40	1.60	1.28	1.14
9	0.28	0.28	0.28	0.28	106-120	2.80	1.80	1.30	1.14
10	0.32	0.32	0.32	0.32	121-125	4.00	1.80	1.30	1.14
11-25	0.64	0.64	0.64	0.64	126-130		2.00	1.30	1.14
26-30	0.84	0.84	0.84	0.64	131-150		2.00	1.40	1.14
31-40	0.84	0.84	0.84	0.84	151-155			1.40	1.14
41	1.04	1.02	1.04	0.84	156-175			1.50	1.14
42-45	1.04	1.04	1.04	0.84	176-200				1.14
46-50	1.14	1.14	1.14	0.84					

228

229 5.2 Model spin-up and simulations

230 All runs in this study needed model spin-up to ensure that the soil moisture of each
 231 HAL reached equilibrium. We found that the spin-up period could last for 50-400 years
 232 for different initial SWC conditions and soil depths in the WRB. When the initial SWC
 233 was set to 0.2 mm³/mm³ with observed soil depths, the spin-up period was about 50
 234 years, which was adopted for production simulations in this study. We performed two
 235 cycles of continuous simulations for 1901-2010. The first cycle was discarded for spin-
 236 up, and the second cycle was retained for analysis.

237

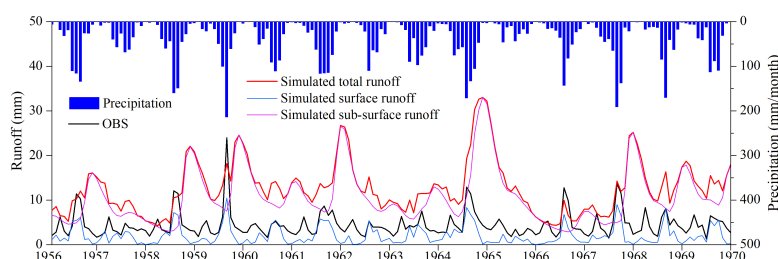
238 6 Results and Analysis

239 6.1 Default runoff simulation

240 We conducted a default run to evaluate the performance of the original CLM5 in
 241 simulating runoff in the WRB. The model remarkably overestimated monthly total and
 242 sub-surface runoff when compared with observations from the BJC hydrological station



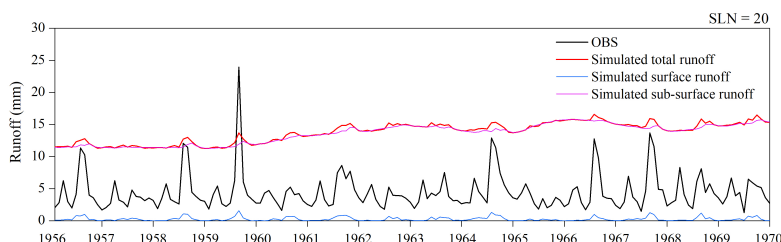
243 over 1956-1969, a period with minimal human activity (Jiao et al., 2017). The
244 correlation coefficient (R^2), root mean square error (RMSE), and Nash Sutcliffe
245 efficiency (NSE) were 0.02, 10.37 mm, and -12.34, respectively. We can see that the
246 overestimation was due mainly to the unrealistic simulations of sub-surface runoff. The
247 reasons for these erroneous simulations are discussed in detail in the following sections.



248
249 Figure 2. Observed monthly precipitation and runoff (black line) and simulated total
250 runoff, surface runoff, and sub-surface runoff in the default run from 1956 to 1969. The
251 observed monthly precipitation is for the entire WRB, and the OBS and simulations are
252 for the BJC hydrological station.
253

254 6.2 Effects of soil depth on runoff simulations

255 We examined how the simulated runoff for the WRB was affected by the actual soil
256 depths (40-197 m) that were inputted into CLM5 with a default SLN of 20. As shown
257 in Figure 3, CLM5 with deep soils greatly suppressed the seasonal variability of sub-
258 surface runoff and reduced the magnitude of surface runoff when compared with the
259 CLM5 simulations with a uniform soil depth of 8 m. The R^2 , RMSE, and NSE between
260 observations and the simulations with actual soil depths were 0.04, 9.8 mm, and -10.96,
261 respectively. Although the actual soil depth data for the WRB were included in CLM5,
262 the runoff simulations were still remarkably different from observations in both
263 variability and magnitude. Hence, the runoff simulations for the WRB need to be further
264 explored and understood.

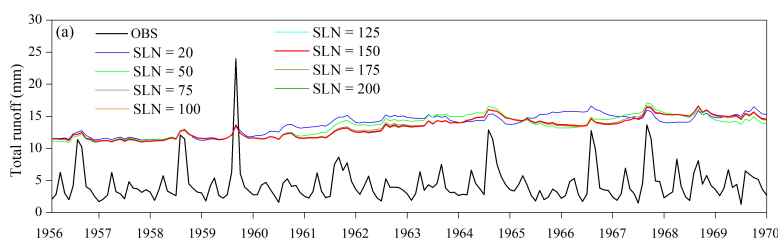


265
266 Figure 3. Observed and simulated total runoff, surface runoff, and sub-surface runoff
267 from 1956 to 1969 by the run with actual soil depths. The SLN was set to 20.

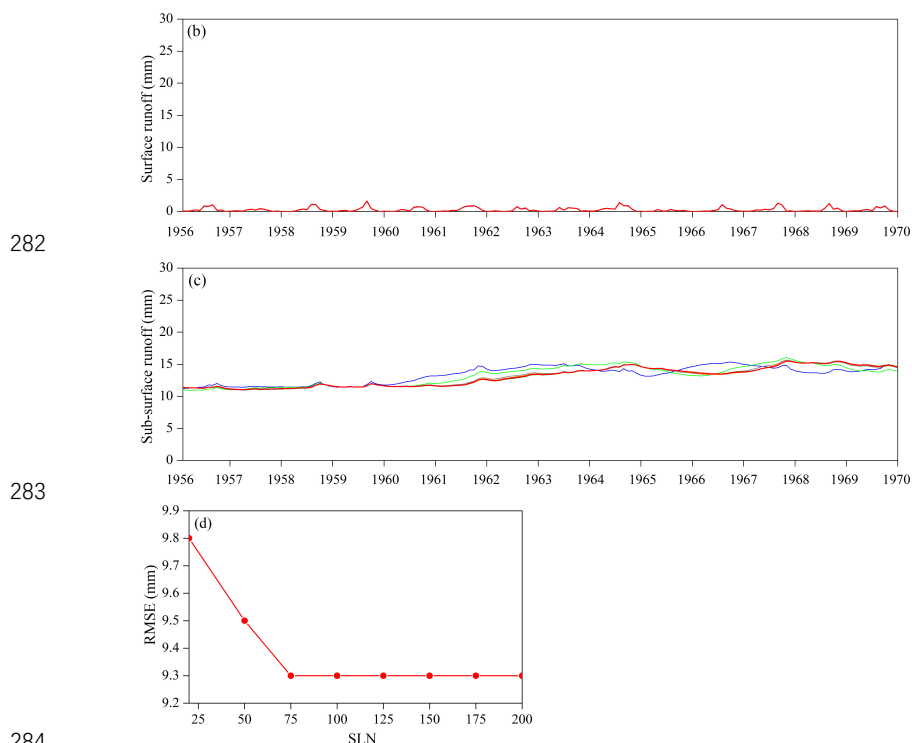
268

269 6.3 Effects of soil layering on runoff simulations

270 The eight soil layering methods mentioned in Section 3.2 were applied to CLM5 with
271 the actual soil depths for the WRB to investigate the effects of soil layering on the runoff
272 simulations. We can see that all the CLM5 runs generated similar temporal patterns of
273 simulated total runoff, as shown in Figure 4a. Obviously, the soil layering methods had
274 almost no effect on the surface runoff simulations (Figure 4b), while these methods did
275 affect the sub-surface runoff simulations to some extent (Figure 4c). When the vertical
276 spatial resolution increased from 20 to 200 soil layers, the RMSE of the simulated total
277 runoff decreased until the SLN was equal to 75, and then the errors reached a minimum
278 for SLN ranging from 100 to 200 (Figure 4d). Although the model with 75 soil layers
279 seemed to be an efficient case, the soil layering method was further examined with
280 vertical soil moisture profile simulations.



281



282

283

284

285

286

287

288

Figure 4. (a) Observed and simulated monthly runoff for the BJC hydrological station; (b) simulated surface runoff; (c) simulated sub-surface runoff; (d) RMSEs of the simulated total runoff. All simulations were produced with different SLN values.

289

290

291

292

293

294

295

296

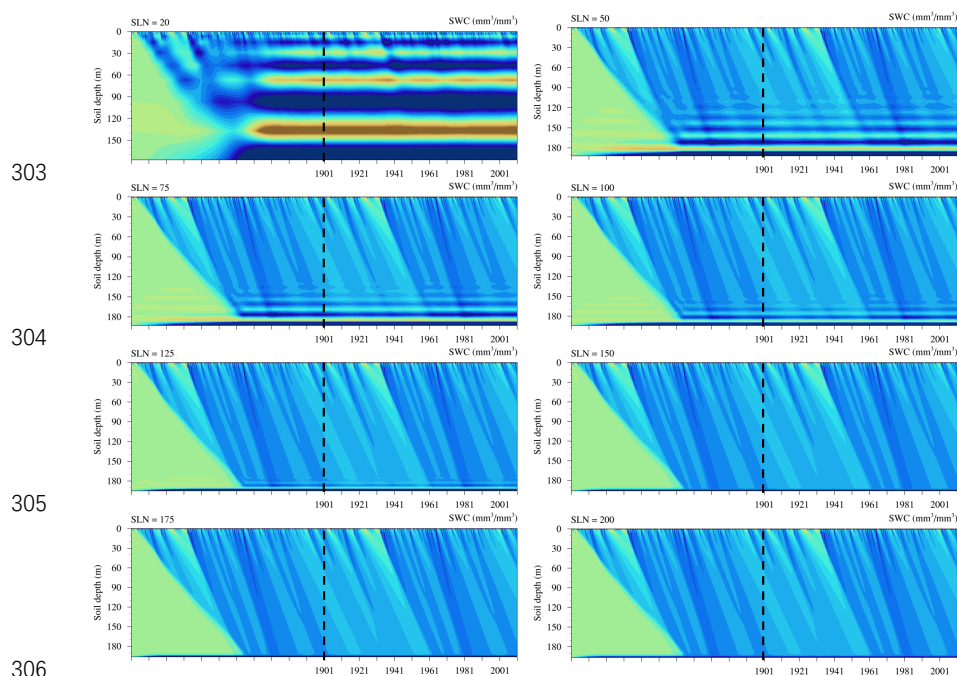
297

298

We selected a point (37.53 °N, 109.33 °E) with the deepest soil depth of 197 m in the WRB to study the soil layering method based on vertical soil moisture profile simulations. As shown in Figure 5, the coarser-resolution simulations ($SLN \leq 125$) resulted in alternating persistent wet-dry layers throughout our study period, and this alternation gradually weakened with increasing SLN. When the SLN was equal to 150, the wet-dry alternation almost disappeared. We examined the model numerical method and found that the coarser resolution numerically caused smaller soil matric potential (SMP) gradients between the soil layers, leading to the wet-dry alternation. These vertical soil moisture simulations indicated that CLM5 could produce smooth soil water flow simulations with at least 150 soil layers at a soil depth of 197 m to avoid these



299 numerical issues, although the RMSE of the simulated total runoff reached the
300 minimum value with SLN equal to 75. Therefore, in the following simulations, we set
301 the model soil layers to 150. With this soil layering, the R^2 , RMSE, and NSE for the
302 total runoff simulations were 0.07, 9.3 mm, and -9.71, respectively.



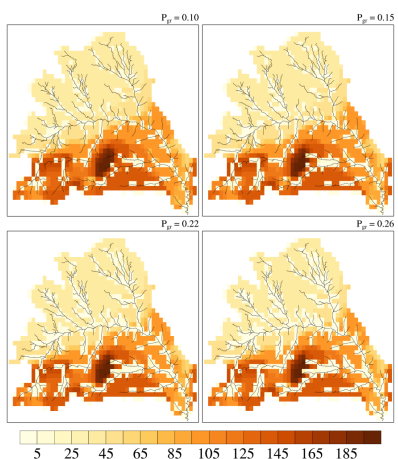
306 Figure 5. Simulated vertical monthly SWC profiles for the selected point in the WRB
307 during both the spin-up (left of the black dashed line) and simulation (right of the black
308 dashed line) periods. All simulations were conducted with different SLN values.
309
310

311 6.4 Effects of P_{gr} on runoff simulations

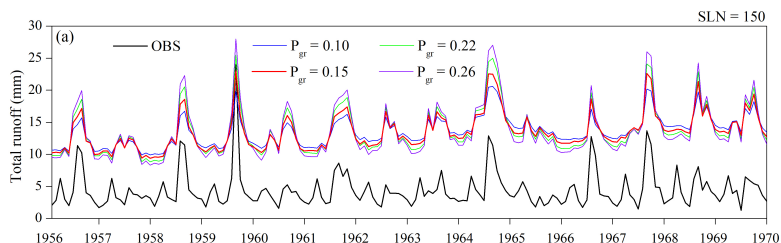
312 In addition to the actual soil depth and high-resolution soil layering, we prescribed the
313 river channels for the WRB in CLM5 to explore the effects of those channels on runoff
314 simulations. Figure 6 shows the spatial distribution of the river channels for the WRB
315 with different values of P_{gr} , a proportion of the total river channel area to the entire
316 WRB area, as previously defined. The larger the P_{gr} , the denser the river channels. Our
317 results showed that CLM5 dramatically improved the simulations of the seasonal
318 variability of total runoff (Figure 7a), and the R^2 increased to 0.41-0.56 from 0.07 for



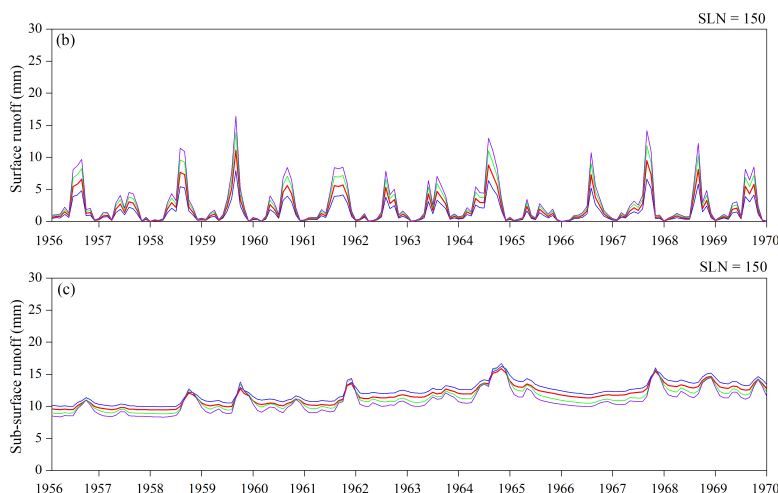
319 the previous simulations. These improvements resulted mainly from the surface runoff
320 simulations with a much higher seasonal variability (Figure 7b). The sub-surface runoff
321 simulations did not show significant changes with the addition of the river channels to
322 CLM5 (Figure 7c). We can see that CLM5 with P_{gr} equal to 0.15 produced the lowest
323 RMSE (9.3 mm) and the highest NSE (-9.78), although the R^2 was not the highest (0.52)
324 with this P_{gr} value. Moreover, we found that the seasonal peak values of the simulated
325 surface runoff with P_{gr} values of 0.22 and 0.26 were higher than the observed peak
326 values (Figure not shown), which was not realistic. Thus, we selected 0.15 for P_{gr} for
327 the rest of our simulations.



328
329 Figure 6. Spatial distributions of river channels (black lines) and soil depths for the
330 WRB with different values of P_{gr} .
331



332



333

334

335

336

337

338

Figure 7. (a) Observed and simulated monthly runoff for the BJC hydrological station; (b) simulated surface runoff; (c) simulated sub-surface runoff. All simulations were produced with different P_{gr} values.

339

Table 2. R^2 , RMSE, and NSE for total runoff simulations with different P_{gr} values

P_{gr}	0.10	0.15	0.22	0.26
R^2	0.41	0.52	0.54	0.56
RMSE (mm)	9.4	9.3	9.4	9.5
NSE	-9.90	-9.78	-10.06	-10.23

340

341 6.5 Water balance analysis

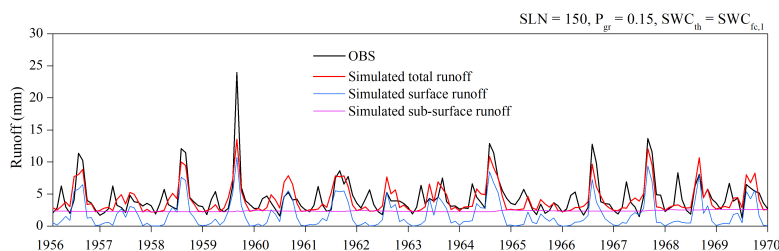
342 We looked into the water balance for the WRB and attempted to further reduce the
 343 biases of the runoff simulations. In the previous sections, the more realistic conditions
 344 of the WRB (actual soil depths, high-resolution soil layering, and river channels) were
 345 incorporated into CLM5 to improve the runoff simulations, but the simulations were
 346 still far away from observations. Tian et al. (2018) indicated that the change in water
 347 storage in the WRB approached zero over a period of 13 years. Our study focused on a
 348 period of 14 years (1956-1969). Thus, we estimated the mean evapotranspiration (ET)
 349 with observed precipitation and runoff over our study period by assuming a water
 350 storage change of zero in the WRB as follows:



351
$$ET_{\text{avg}} = P_{\text{avg}} - R_{\text{avg}} \quad (1)$$

352 where ET_{avg} , P_{avg} , and R_{avg} are mean ET (mm), precipitation (mm), and runoff (mm)
353 over 1956-1969, respectively. Here, P_{avg} is 454.7 mm, R_{avg} is 53.2 mm, and the
354 estimated ET_{avg} is 401.5 mm. However, the simulated mean ET over the study period
355 was 267.8 mm, which was far below the estimated value. According to the soil
356 evaporation parameterization in CLM5, when the SWC of the top soil layer (SWC_1)
357 was less than SWC_{th} , a DSL formed to resist soil evaporation. In CLM5, the SWC_{th} is
358 defined as 80% of $SWC_{\text{sat},1}$. However, previous studies (Lee and Pielke, 1992;
359 Sakaguchi and Zeng, 2009; Flammini et al., 2018) found that soil evaporation starts to
360 decrease significantly when the surface SWC is less than the field capacity. Yang et al.
361 (1985) also found that soil evaporation in the LP slows down when the surface SWC
362 becomes lower than a stable capacity that is close to the field capacity. Thus, in this
363 study, we changed the SWC_{th} to the $SWC_{\text{fc},1}$ to conduct one additional simulation. With
364 this modification, the simulated annual ET fluctuated around the estimated mean ET
365 for our study period (401.5 mm), and the simulated 14-year mean value was 392.5 mm,
366 which was close to the estimated mean. Very importantly, the simulated total runoff
367 drastically reduced to match observations by increasing ET (Figure 8). When compared
368 with those for the simulations in the last section, R^2 increased from 0.52 to 0.62, RMSE
369 decreased from 9.3 to 1.8 mm, and NSE increased dramatically from -9.78 to 0.61.
370 Therefore, we remarkably improved runoff simulations with more accurate ET
371 simulations in addition to the more realistic WRB features.

372



373
374 Figure 8. Time series of observed monthly runoff (black line) for the BJC hydrological
375 station and simulated monthly total (red line), surface (blue line), and sub-surface
376 runoff (pink line).
377

378 7 Conclusions and discussion

379 This study was intended to improve runoff simulations with CLM5 for the complex
380 topography of the WRB and to improve our understanding of deep soil hydrological
381 processes. In CLM5, we included actual soil depths for the WRB ranging from 0 to 197
382 m and added the river channels for this watershed. We tested eight soil layering methods
383 and found that CLM5 with at least 150 soil layers could produce rational simulations
384 for both runoff and the vertical soil moisture profile. Different values of river channel
385 density were examined with CLM5, showing that a ratio of 15% of the total river
386 channel area to the entire WRB area generated the most reasonable results.

387

388 With the above model settings, our simulations showed that CLM5 with actual soil
389 depths greatly suppressed the seasonal variability of simulated sub-surface runoff and
390 reduced the simulated surface runoff when compared with the default simulations with
391 a uniform soil depth of 8 m. In addition, CLM5 with finer-resolution soil layering (SLN
392 ≥ 150) led to more accurate runoff and smoother vertical soil water flow simulations
393 than that with coarser-resolution layering, and the latter was consistent with the
394 homogeneous distribution of vertical soil texture in the WRB. The addition of river
395 channels for the WRB to CLM5 significantly increased the seasonal variability of
396 simulated surface runoff, remarkably improving the seasonal variability of simulated



397 total runoff. Moreover, more accurate simulations of soil evaporation in the WRB
398 dramatically reduced the simulated sub-surface runoff and improved the total runoff
399 simulations.

400

401 Limitations still exist in this study. We used atmospheric forcing data at a 5 km
402 resolution to drive CLM5, but for our study region with very complex terrain, this
403 resolution may not be sufficient and could potentially have generated errors in our
404 simulations. In the meantime, it is very important to expand this study to a larger or
405 even global scale, and accurate soil depth and detailed soil texture data would be vital
406 to such an expanded study. In addition, soil hydraulic properties may change with depth,
407 but this study did not consider such changes, and this needs to be tested in future studies.
408 Despite these limitations, it is clear that our final runoff simulations with an improved
409 CLM5 were highly accurate, and our understanding of deep soil hydrological processes
410 has advanced.

411

412 Author contributions. JJ and LW designed the research; LW conducted the simulations;
413 LW and JY collected the soil depth data; JJ and LW analyzed the data; JY was involved
414 in several sensitivity simulation tests; JJ and LW wrote the paper; BS and GN edited
415 the paper and provided substantial comments for scientific clarification.

416

417 Code and data availability. Our improved model and data are available at
418 <https://doi.org/10.5281/zenodo.5044541>.

419

420 Competing interests. The authors declare that they have no conflict of interest.

421



422 Acknowledgments. This research was funded by the National Natural Science
423 Foundation of China (No. 41571030, No. 91637209, and No. 91737306).

424

425 References

- 426 Camacho, V. V., Saraiva Okello, A. M. L., Wenninger, J. W., and Uhlenbrook, S.:
427 Understanding runoff processes in a semi-arid environment through isotope and
428 hydrochemical hydrograph separations, *Hydrol. Earth Syst. Sci. Discuss.*, 19,
429 4183-4199, <https://doi.org/10.5194/hessd-12-975-2015>, 2015.
- 430 Chen, L., Sela, S., Svoray, T., and Assouline, S.: The role of soil-surface sealing,
431 microtopography, and vegetation patches in rainfall-runoff processes in semiarid
432 areas, *Water Resour. Res.*, 49, 5585-5599, 2013.
- 433 Clapp, R. B. and Hornberger, G. M.: Empirical equations for some soil hydraulic
434 properties, *Water Resour. Res.*, 14, 601-604, 1978.
- 435 Cosby, B. J., Hornberger, G. M., Clapp, R. B., and Ginn, T. R.: A statistical exploration
436 of the relationships of soil moisture characteristics to the physical properties of
437 soils, *Water Resour. Res.*, 20, 682-690, 1984.
- 438 Cressman, G. P.: An operational objective analysis system, *Mon. Weather Rev.*, 87, 367-
439 374, 1959.
- 440 Döll, P. and Fiedler, K.: Global-scale modeling of groundwater recharge, *Hydrol. Earth*
441 *Syst. Sci. Discuss.*, 12, 863-885, <https://doi.org/10.5194/hess-12-863-2008>,
442 2008.
- 443 Ek, M. B., Mitchell, K. E., Lin, Y., Rogers, E., Grunmann, P., Koren, V., Gayno, G., and
444 Tarpley, J., D.: Implementation of Noah land surface model advances in the
445 National Centers for Environmental Prediction operational mesoscale Eta model,
446 *J. Geophys. Res.*, 108, 8851, <https://doi.org/10.1029/2002JD003296>, 2003.
- 447 Flammini, A., Corradini, C., Morbidelli, R., Saltalippi, C., Picciafuoco, T., and Giráldez,
448 J. V.: Experimental analyses of the evaporation dynamics in bare soils under
449 natural conditions, *Water Resour. Manag.*, 32, 1153-1166,
450 <https://doi.org/10.1007/s11269-017-1860-x>, 2018.
- 451 Fu, B.: Soil erosion and its control in the Loess Plateau of China, *Soil Use Manage.*, 5,
452 76-82, 1989.
- 453 Fu, B., Wang, S., Liu, Y., Liu, J., Liang, W., and Miao, C.: Hydrogeomorphic Ecosystem
454 Responses to Natural and Anthropogenic Changes in the Loess Plateau of China,
455 *Annu. Rev. Earth Planet. Sci.*, 45, 223-243, <https://doi.org/10.1146/annurev-earth-063016-02055>, 2017.
- 457 Fu, Z., Li, Z., Cai, C., Shi, Z., Xu, Q., and Wang, X.: Soil thickness effect on
458 hydrological and erosion characteristics under sloping lands: A hydrogeological
459 perspective, *Geoderma*, 167-168, 41-53,
460 <https://doi.org/10.1016/j.geoderma.2011.08.013>, 2011.
- 461 Han, S., Li, Y., Shi, Y., Yang, X., Zhang, X., and Shi, Z.: The characteristic of soil
462 moisture resources on the Loess Plateau, *Bulletin of Soil and Water Conservation*,
463 10, 36-43, 1990.
- 464 Huang, T. and Pang, Z.: Estimating groundwater recharge following land-use change
465 using chloride mass balance of soil profiles: A case study at Guyuan and Xifeng
466 in the Loess Plateau of China, *Hydrogeology J.*, 19, 177-186,
467 <https://doi.org/10.1007/s10040-010-0643-8>, 2011.



- 468 Huang, T., Pang, Z., and Edmunds, W. M.: Soil profile evolution following land-use
469 change: Implications for groundwater quantity and quality, *Hydrol. Process.*, 27,
470 1238-1252, <https://doi.org/10.1002/hyp.9302>, 2013.
- 471 Huang, T., Pang, Z., Liu, J., Yin, L., and Edmunds, W. M.: Groundwater recharge in an
472 arid grassland as indicated by soil chloride profile and multiple tracers, *Hydrol.*
473 *Process.*, 31, 1047-1057, <https://doi.org/10.1002/hyp.11089>, 2017.
- 474 Huang, Y., Evaristo, J., and Li, Z.: Multiple tracers reveal different groundwater
475 recharge mechanisms in deep loess deposits, *Geoderma*, 353, 204-212,
476 <https://doi.org/10.1016/j.geoderma.2019.06.041>, 2019.
- 477 Jencso, K. G. and Mcglynn, B. L.: Hierarchical controls on runoff generation:
478 Topographically driven hydrologic connectivity, geology, and vegetation, *Water*
479 *Resour. Res.*, 47, W11527, 2011.
- 480 Jiao, Y., Lei, H., Yang, D., Huang, M., Liu, D., and Yuan, X.: Impact of vegetation
481 dynamics on hydrological processes in a semi-arid basin by using a land surface-
482 hydrology coupled model, *J. Hydrol.*, 551, 116-131,
483 <https://doi.org/10.1016/j.jhydrol.2017.05.060>, 2017.
- 484 Jing, K. and Cheng, Y.: Preliminary study of the erosion environment and rates on the
485 Loess Plateau, *Geogr. Res.*, 2, 1-11, 1983.
- 486 Lawrence, D., Fisher, R., Koven, C., Oleson, K., Swenson, S., Vertenstein, M., Andre,
487 B., Bonan, G., Ghimire, B., Kampenhout, L. V., Kennedy, D., Kluzek, E., Knox,
488 R., Lawrence, P., Li, F., Li, H., Lombardozzi, D., Lu, Y., Perket, J., Riley, W., Sacks,
489 W., Shi, M., Wieder, W., Xu, C., Ali, A., Badger, A., Bisht, G., Broxton, P., Brunke,
490 M., Buzan, J., Clark, M., Craig, T., Dahlin, K., Drewniak, B., Emmons, L., Fisher,
491 J., Flanner, M., Gentine, P., Lenaerts, J., Levis, S., Leung, L. R., Lipscomb, W.,
492 Pelletier, J., Ricciuto, D. M., Sanderson, B., Shuman, J., Slater, A., Subin, Z., Tang,
493 J., Tawfik, A., Thomas, Q., Tilmes, S., Vitt, F., and Zeng, X.: Technical Description
494 of version 5.0 of the Community Land Model (CLM5), National Center for
495 Atmospheric Research, Boulder, Colorado, 2018.
- 496 Lawrence, D. M. and Slater, A. G.: Incorporating organic soil into a global climate
497 model, *Clim. Dynam.*, 30, 145-160, <https://doi.org/10.1007/s00382-007-0278-1>,
498 2008.
- 499 Lawrence, P. J. and Chase, T. N.: Representing a new MODIS consistent land surface
500 in the Community Land Model (CLM5 3.0), *J. Geophys. Res.*, 112, G01023, 2007.
- 501 Lee, T. J. and Pielke, R. A.: Estimating the soil surface specific humidity, *J. Appl.*
502 *Meteorol.*, 31, 480-484, 1992.
- 503 Lei, X.: Pore types and collapsibility of the loess in China, Science China Press, 1203-
504 1208, 1987.
- 505 Li, Y., Han, S. and Wang, Z.: Soil water properties and its zonation in the Loess Plateau.
506 *Res. Soil Water Conserv.*, 1-17, 1985.
- 507 Li, Z., Chen, X., Liu, W., and Si, B.: Determination of groundwater recharge
508 mechanism in the deep loessial unsaturated zone by environmental tracers, *Sci*
509 *Total Environ*, 586, 827-835, <https://doi.org/10.1016/j.scitotenv.2017.02.061>,
510 2017.
- 511 Li, Z., Jasechko, S., and Si, B.: Uncertainties in tritium mass balance models for
512 groundwater recharge estimation, *J. Hydrol.*, 571, 150-158,
513 <https://doi.org/10.1016/j.jhydrol.2019.01.030>, 2019.
- 514 Liu, D., Tian, F., Hu, H., and Hu, H.: The role of run-on for overland flow and the
515 characteristics of runoff generation in the Loess Plateau, China, *Hydrol. Sci. J.*, 57,
516 1107-1117, 2012.
- 517 Liu, Z.: The Study on the Classification of Loess Landscape and the Characteristics of



- 518 Loess Stratum, M.S. thesis, College of Geological Engineering and Geomatics,
519 Chang'an University, China, 2016.
- 520 Neitsch, S. L., Arnold, J. G., Kiniry, J. R., and Williams, J. R.: Soil and Water
521 Assessment Tool Theoretical Documentation Version 2009. Texas Water
522 Resources Institute Technical Report, Texas, 2011.
- 523 Niu, G. Y., Yang, Z. L., Dickinson, R. E., and Gulden, L. E.: A simple TOPMODEL-
524 based runoff parameterization (SIMTOP) for use in global climate models, *J.*
525 *Geophys. Res.*, 110, D21106, 2005.
- 526 Niu, G., Yang, Z., Mitchell, K. E., Chen, F., Ek, M. B., Barlage, M., Kumar, A.,
527 Manning, K., Niyogi, D., Rosero, E., Tewari, M., and Xia, Y.: The community
528 Noah land surface model with multiparameterization options (Noah-MP): 1.
529 Model description and evaluation with local-scale measurements, *J. Geophys. Res.*,
530 116, D12109, <https://doi.org/10.1029/2010JD015139>, 2011.
- 531 Qi, C., Gan, Z., Xi, Z., Wu, C., Sun, H., Chen, W., Liu, T., and Zhao, G.: The research
532 of the relations between erosion landforms and soil erosion of the Loess Plateau,
533 Shaanxi People's Education Publishing House, Shaanxi, China, 1991.
- 534 Sakaguchi, K. and Zeng, X.: Effects of soil wetness, plant litter, and under-canopy
535 atmospheric stability on ground evaporation in the Community Land Model
536 (CLM53. 5), *J. Geophys. Res.*, 114, 2009.
- 537 Saraiva Okello, A. M. L., Uhlenbrook, S., Jewitt, G. P. W., Masih, I., Riddell, E. S., and
538 Van der Zaag, P.: Hydrograph separation using tracers and digital filters to quantify
539 runoff components in a semi-arid mesoscale catchment, *Hydrol. Process.*, 32,
540 1334-1350, <https://doi.org/10.1002/hyp.11491>, 2018.
- 541 Shangguan, W., Hengl, T., Mendes de Jesus, J., Yuan, H., and Dai, Y.: Mapping the
542 global depth to bedrock for land surface modeling, *J. Adv. Model. Earth Syst.*, 9,
543 65-88, <https://doi.org/10.1002/2016MS000686>, 2017.
- 544 Shao, J., Si, B., and Jin, J.: Extreme precipitation years and their occurrence frequency
545 regulate long-term groundwater recharge and transit time, *Vadose Zone J.*, 17, 1-
546 9, <https://doi.org/10.2136/vzj2018.04.0093>, 2018.
- 547 Swenson, S. C. and Lawrence, D. M.: Assessing a dry surface layer-based soil
548 resistance parameterization for the Community Land Model using GRACE and
549 FLUXNET-MTE data, *J. Geophys. Res. Atmos.*, 119, 10,299-10,312, 2014.
- 550 Tesfa, T. K., Tarboton, D. G., Chandler, D. G., and McNamara, J. P.: Modeling soil
551 depth from topographic and land cover attributes, *Water Resour. Res.*, 45, W10438,
552 2009.
- 553 Tian, L., Jin, J., Wu, P., and Niu, G.: Assessment of the effects of climate change on
554 evapotranspiration with an improved elasticity method in a nonhumid area,
555 *Sustainability*, 10, 4589, <https://doi.org/10.3390/su10124589>, 2018.
- 556 Turkeltaub, T., Kurtzman, D., Bel, G., and Dahan, O.: Examination of groundwater
557 recharge with a calibrated/validated flow model of the deep vadose zone, *J.*
558 *Hydrol.*, 522, 618-627, <https://doi.org/10.1016/j.jhydrol.2015.01.026>, 2015.
- 559 Uhlenbrook, S., Frey, M., Leibundgut, C., and Maloszewski, P.: Hydrograph
560 separations in a mesoscale mountainous basin at event and seasonal timescales,
561 *Water Resour. Res.*, 38, 1096, 2002.
- 562 Wang, S.: Study on geological engineering of loess in North Shaanxi, M. S. thesis,
563 College of Geological Engineering and Geomatics, Chang'an University, China,
564 2016.
- 565 Wang, Y. and Shao, M.: Spatial variability of soil physical properties in a region of the
566 Loess Plateau of pr China subject to wind and water erosion, *Land Degrad. Dev.*,
567 24, 296-304, <https://doi.org/10.1002/ldr.1128>, 2013.



- 568 Xiang, W., Si, B., Biswas, A., and Li, Z.: Quantifying dual recharge mechanisms in
569 deep unsaturated zone of Chinese Loess Plateau using stable isotopes, *Geoderma*,
570 337, 773-781, <https://doi.org/10.1016/j.geoderma.2018.10.006>, 2019.
- 571 Xiao, J., Wang, L., Deng, L., and Jin, Z.: Characteristics, sources, water quality and
572 health risk assessment of trace elements in river water and well water in the
573 Chinese Loess Plateau, *Sci. Total Environ.*, 650, 2004-2012,
574 <https://doi.org/10.1016/j.scitotenv.2018.09.322>, 2019.
- 575 Yang, W., Shi, Y., and Fei, W.: Water evaporation from soils under unsaturated condition
576 and evaluation for drought resistance of soils on Loessal Plateau, *Acta Pedologica*
577 *Sinica*, 22, 13-23, 1985.
- 578 Zhang, F., Zhang, W., Qi, J., and Li, F.: A regional evaluation of plastic film mulching
579 for improving crop yields on the Loess Plateau of China, *Agric. For. Meteorol.*,
580 248, 458-468, <https://doi.org/10.1016/j.agrformet.2017.10.030>, 2018.
- 581 Zhu, Y., Jia, X., and Shao, M.: Loess thickness variations across the Loess Plateau of
582 China, *Surv. Geophys.*, 39, 715-727, <https://doi.org/10.1007/s10712-018-9462-6>,
583 2018.